Atmospheric Chemistry of n-$C_6F_{13}CH_2CHO$: Formation from n-$C_6F_{13}CH_2CH_2OH$, Kinetics, and Mechanisms of Reactions with Chlorine Atoms and OH Radicals

Malisa S. Chiappero and Gustavo A. Argüello

INFIQC, Departamento de Físico Química, Facultad de Ciencias Químicas, Universidad Nacional de Córdoba, Ciudad Universitaria, 5000 Córdoba, Argentina

M. D. Hurley and T. J. Wallington*

Ford Motor Company, Mail Drop SRL-3083, Dearborn, Michigan 48121

Received: February 22, 2010; Revised Manuscript Received: April 6, 2010

Smog chamber FTIR techniques were used to measure $k(Cl + n\text{-}C_6F_{13}CH_2CHO) = (1.84 \pm 0.22) \times 10^{-11}$, $k(Cl + n\text{-}C_6F_{13}CHO) = (1.75 \pm 0.70) \times 10^{-12}$, and $k(OH + n\text{-}C_6F_{13}CH_2CHO) = (2.15 \pm 0.26) \times 10^{-12}$ cm^3 molecule^{-1} s^{-1} in 700 Torr of N_2 or air diluent at 296 ± 2K. The chlorine-atom-initiated oxidation of n-$C_6F_{13}CH_2CH_2OH$ in air gives n-$C_6F_{13}CH_2CHO$ in a molar yield of 99 ± 8%. The atmospheric fate of n-$C_6F_{13}CH_2C(O)$ radicals is reaction with O_2, while the fate of n-$C_6F_{13}C(O)$ radicals is decomposition to give n-C_6F_{13} radicals and CO. The results are discussed with respect to the atmospheric chemistry of fluorinated alcohols and the formation of perfluorocarboxylic acids.

1. Introduction

Fluorinated alcohols are used in a variety of industrial applications (e.g., paints, coatings, polymers, adhesives, waxes, polishes, electronic materials, caulks), and detailed information on their environmental impact is needed. There is interest in the atmospheric oxidation processes that may convert fluorinated alcohols to perfluorinated carboxylic acids (PFCAs) of the form $C_nF_{2n+1}C(O)OH$. PFCAs are persistent in the environment, resisting degradation via oxidation, hydrolysis, or reduction under biotic and abiotic conditions.[1] Analysis of rainwater indicates the widespread distribution of short-chain PFCAs ($n = 2-7$) at low levels (~1−100 ng/L).[2] Long-chain PFCAs are bioaccumulative[3] and have been observed in fish from the Great Lakes[4] and in Arctic fish and mammals.[5]

Fluorotelomer alcohols (FTOHs) are a class of fluorinated alcohols that have been suggested[6,7] as plausible sources of PFCAs in remote locations. FTOHs are linear fluorinated alcohols with the formula $C_nF_{2n+1}CH_2CH_2OH$ ($n = 2, 4, 6, ...$). Fluorotelomer alcohols are volatile, have been detected in the air over North America, Arctic, Europe, Japan, and off of the West African coast,[8−11] have an atmospheric lifetime (approximately 10−20 days) sufficient for widespread hemispheric distribution,[6,12] and undergo atmospheric oxidation in the absence of NO_x to give perfluorocarboxylic acids.[7,13]

Most studies of fluorinated alcohols have concentrated on smaller members of the class (e.g., $CF_3CH_2CH_2OH$) because they are easy to handle and appropriate reference standards (e.g., CF_3CH_2CHO and CF_3CHO) are commercially available. It is generally assumed that the chemistry of the larger, more commercially relevant alcohols is the same as that of the smaller members of the series. Results from our recent study of n-$C_8F_{17}CH_2CH_2OH$ and n-$C_8F_{17}CH_2CHO$ oxidation[14] provide support for this assumption. To provide further insight into the atmospheric chemistry of fluorotelomer alcohols, we have conducted a study of the atmospheric chemistry of n-$C_6F_{13}CH_2CHO$. All species considered in the present work are the linear isomers, and we drop the "n-" suffix from here on. The photochemistry of $C_6F_{13}CH_2CHO$ has been reported by two different groups[15,16] and is discussed elsewhere. In the present study, we investigate the formation of $C_6F_{13}CH_2CHO$ from the oxidation of $C_6F_{13}CH_2CH_2OH$, the kinetics of the chlorine-atom- and OH-radical-initiated oxidation of $C_6F_{13}CH_2CHO$, and the atmospheric fate of $C_6F_{13}CH_2C(O)$ and $C_6F_{13}C(O)$ radicals.

2. Experimental Section

Experiments were performed in a 140 L Pyrex reactor interfaced to a Mattson Sirius 100 FTIR spectrometer.[17] The reactor was surrounded by 22 fluorescent blacklamps (GE F15T8-BL), which were used to initiate the experiments. Chlorine atoms were produced by photolysis of molecular chlorine.

$$Cl_2 + h\nu \rightarrow Cl + Cl \quad (1)$$

OH radicals were produced by the photolysis of CH_3ONO in air

$$CH_3ONO + h\nu \rightarrow CH_3O + NO \quad (2)$$

$$CH_3O + O_2 \rightarrow HO_2 + HCHO \quad (3)$$

$$HO_2 + NO \rightarrow OH + NO_2 \quad (4)$$

Relative rate techniques were used to measure the rate constant of interest relative to a reference reaction whose rate constant has been established previously. The relative rate method is a well-established technique[18] for measuring the reactivity of Cl atoms and OH radicals with organic compounds. Kinetic data are derived by monitoring the loss of a reactant compound

* To whom correspondence should be addressed. E-mail: twalling@ford.com.

10.1021/jp101587m
Published on Web 04/30/2010

relative to one or more reference compounds. The decays of the reactant and reference are then plotted using the expression

$$\ln\left(\frac{[\text{reactant}]_{t_0}}{[\text{reactant}]_t}\right) = \frac{k_{\text{reactant}}}{k_{\text{reference}}} \ln\left(\frac{[\text{reference}]_{t_0}}{[\text{reference}]_t}\right) \qquad \text{(I)}$$

where $[\text{reactant}]_{t_0}$, $[\text{reactant}]_t$, $[\text{reference}]_{t_0}$, and $[\text{reference}]_t$ are the concentrations of the reactant and reference at times t_0 and t and k_{reactant} and $k_{\text{reference}}$ are the rate constants for reactions of Cl atoms or OH radicals with the reactant and reference. Plots of $\ln([\text{reactant}]_{t_0}/[\text{reactant}]_t)$ versus $\ln([\text{reference}]_{t_0}/[\text{reference}]_t)$ should be linear, pass through the origin, and have a slope of $k_{\text{reactant}}/k_{\text{reference}}$.

$C_6F_{13}CH_2CHO$ and $C_6F_{13}CH_2CH_2OH$ were monitored by FTIR spectroscopy using an infrared path length of 27 m and a resolution of 0.25 cm^{-1}. Infrared spectra were derived from 32 coadded interferograms. All experiments were performed at 700 Torr and 296 ± 2 K. Liquid reagents were introduced into the chamber by transferring their vapor above the liquid via a calibrated volume. Similarly, gaseous reagents were introduced into the chamber via a calibrated volume. The contents of the calibrated volume were swept into the chamber with the diluent gas (air or nitrogen). With the exception of $C_6F_{13}CH_2CHO$, all reagents were obtained from commercial sources (with purities > 99%). A sample of $C_6F_{13}CH_2CHO$ was obtained from P&M-Invest with a stated purity of >97%. All reagents were subjected to repeated freeze/pump/thaw cycling before use. Ultrahigh-purity synthetic air and nitrogen from Michigan Airgas were used as diluent gases.

Initial reagent concentrations for Cl atom relative rate experiments were 3.2 mTorr of $C_6F_{13}CH_2CHO$, 3−14 mTorr of the reference compound (C_2H_5Cl or CH_3OH), and 100 mTorr of Cl_2 in 700 Torr of N_2 diluent. Initial reagent concentrations for OH radical relative rate experiments were 3−6 mTorr of $C_6F_{13}CH_2CHO$, 3−8 mTorr of C_2H_4, and 100 mTorr of CH_3ONO in 700 Torr of air diluent. Reactant and reference compounds were monitored using absorption features over the following wavenumber ranges (cm^{-1}): $C_6F_{13}CH_2CH_2OH$, 700−1200; $C_6F_{13}CH_2CHO$, 600−1800; C_2H_4, 900−1000; C_2H_5Cl, 920−1320; and CH_3OH, 1000−1100. Unless stated otherwise, quoted uncertainties include two standard deviations from least-squares regressions and uncertainties in the analysis of the IR spectra (typically ±1% of original concentrations of the reactants).

3. Results

3.1. Relative Rate Study of $k(Cl + C_6F_{13}CH_2CHO)$. The rate of reaction 5 was measured relative to reactions 6 and 7.

$$Cl + C_6F_{13}CH_2CHO \rightarrow \text{products} \qquad (5)$$

$$Cl + C_2H_5Cl \rightarrow \text{products} \qquad (6)$$

$$Cl + CH_3OH \rightarrow \text{products} \qquad (7)$$

Figure 1 shows the loss of $C_6F_{13}CH_2CHO$ versus the reference compounds following the UV irradiation of $C_6F_{13}CH_2CHO$/reference/Cl_2 mixtures in 700 Torr of N_2 diluent. The lines through the data in Figure 1 are linear least-squares fits, which give $k_5/k_6 = 2.33 \pm 0.25$ and $k_5/k_7 = 0.33 \pm 0.03$. Using literature data[19,20] for $k_6 = 8.0 \times 10^{-12}$ and $k_7 = 5.5 \times 10^{-11}$,

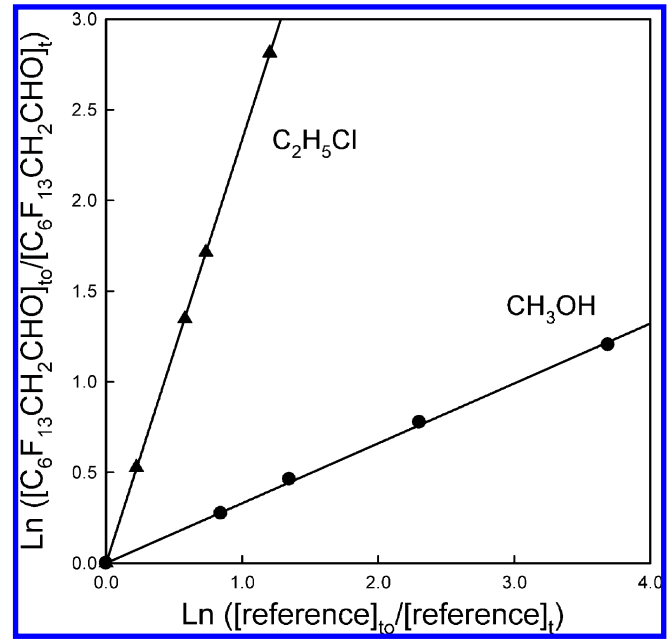

Figure 1. Loss of $C_6F_{13}CH_2CHO$ versus the reference compounds (C_2H_5Cl or CH_3OH) following exposure to chlorine atoms in 700 Torr of N_2.

we derive $k_5 = (1.86 \pm 0.20) \times 10^{-11}$ and $(1.81 \pm 0.16) \times 10^{-11}$ cm^3 $molecule^{-1}$ s^{-1}. Results obtained using the two different reference compounds were, within the experimental uncertainties, indistinguishable. We cite a final value for k_5 which is the average of the two determinations together with error limits which encompass the extremes of the individual determinations, $k_5 = (1.84 \pm 0.22) \times 10^{-11}$ cm^3 $molecule^{-1}$ s^{-1}.

Chiappero et al.[14] reported $k(Cl + C_8F_{17}CH_2CHO) = (1.9 \pm 0.4) \times 10^{-11}$ cm^3 $molecule^{-1}$ s^{-1}. Kelly et al.[21] reported data which when scaled using $k(Cl + HC(O)OC_2H_5) = 1.03 \times 10^{-11}$ [22] gave $k(Cl + CF_3CH_2CHO) = (1.98 \pm 0.03) \times 10^{-11}$ cm^3 $molecule^{-1}$ s^{-1}. Hurley et al.[23,24] reported $k(Cl + CF_3CH_2CHO) = (1.81 \pm 0.27) \times 10^{-11}$ and $k(Cl + C_4F_9CH_2CHO) = (1.84 \pm 0.30) \times 10^{-11}$ cm^3 $molecule^{-1}$ s^{-1}. The rates of the reactions of $C_nF_{2n+1}CH_2CHO$ ($n = 1$, 4, 6, and 8) toward chlorine atoms are indistinguishable within the experimental uncertainties. This observation is consistent with the expectation that the majority of the reaction occurs via abstraction of the aldehydic hydrogen atom, which will not be impacted substantially by the size of the C_nF_{2n+1} group.

3.2. Relative Rate Study of the Reaction of OH Radicals with $C_6F_{13}CH_2CHO$. The rate of reaction 8 was measured relative to reaction 9.

$$OH + C_6F_{13}CH_2CHO \rightarrow \text{products} \qquad (8)$$

$$OH + C_2H_4 \rightarrow \text{products} \qquad (9)$$

Figure 2 shows the loss of $C_6F_{13}CH_2CHO$ versus C_2H_4 following the UV irradiation of a mixture of 6.2 mTorr of $C_6F_{13}CH_2CHO$, 2.4 mTorr of C_2H_4, and 100 mTorr of CH_3ONO in 700 Torr of air diluent. The line through the data is a linear least-squares fit which gives $k_8/k_9 = 0.25 \pm 0.03$, which using $k_9 = 8.66 \times 10^{-12}$ [25] yields $k_8 = (2.15 \pm 0.26) \times 10^{-12}$ cm^3 $molecule^{-1}$ s^{-1}. Sellevåg et al.,[26] Kelly et al.,[21] and Hurley et al.[23] have studied the reactivity of OH radicals toward CF_3CH_2CHO and report

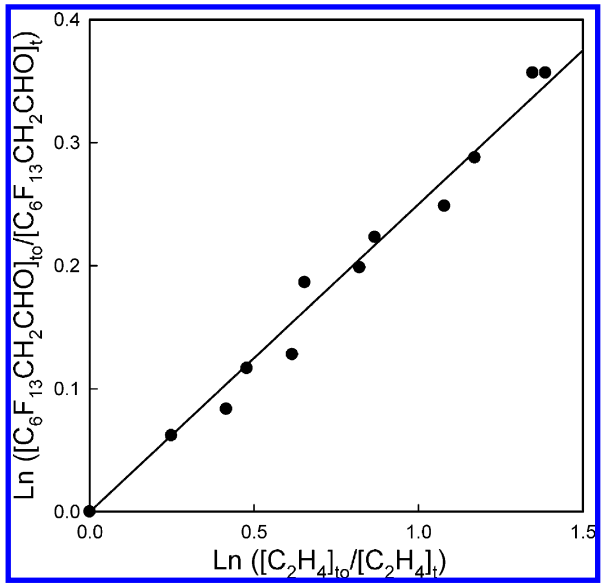

Figure 2. Loss of $C_6F_{13}CH_2CHO$ versus C_2H_4 following exposure to hydroxyl radicals in 700 Torr of air.

$k(OH + CF_3CH_2CHO) = (3.6 \pm 0.3) \times 10^{-12}$, $(2.96 \pm 0.04) \times 10^{-12}$, and $(2.57 \pm 0.44) \times 10^{-12}$ cm^3 molecule^{-1} s^{-1}, respectively. Chiappero et al.[14] reported $k(OH + C_8F_{17}CH_2CHO) = (2.0 \pm 0.4) \times 10^{-12}$ cm^3 molecule^{-1} s^{-1} in 700 Torr of air diluent at 296 ± 2 K. As with the chlorine atom reactions, there is no evidence for a dependence of the reactivity of OH radicals with $C_nF_{2n+1}CH_2CHO$ on the size of the C_nF_{2n+1} group. Taking an average of the available determinations (except that from Sellevåg et al.[26]) gives $k(OH + C_nF_{2n+1}CH_2CHO) = 2.4 \times 10^{-12}$ cm^3 molecule^{-1} s^{-1}.

3.3. Formation of $C_6F_{13}CH_2CHO$ in the Cl-Atom-Initiated Oxidation of $C_6F_{13}CH_2CH_2OH$. Figure 3 shows IR spectra recorded before (A) and after (B) a 12 s irradiation of a mixture of 6.8 mTorr of $C_6F_{13}CH_2CH_2OH$ and 100 mTorr of Cl_2 in 700 Torr of air. Panel C is the product spectrum obtained by subtracting features attributable to $C_6F_{13}CH_2CH_2OH$ from panel B. The consumption of $C_6F_{13}CH_2CH_2OH$ was 24%. Panel D is a reference spectrum of the aldehyde $C_6F_{13}CH_2CHO$. It is clear from comparison of panels C and D that $C_6F_{13}CH_2CHO$ is a major product in the system. Figure 4 shows a plot of the observed $C_6F_{13}CH_2CHO$ formation versus the $C_6F_{13}CH_2CH_2OH$ loss. Assuming that $C_6F_{13}CH_2CHO$ is formed following reaction 10 and is lost solely via reaction 5, then its concentration profile can be described by expression eq II[27]

$$\frac{[C_6F_{13}CH_2CHO]}{[C_6F_{13}CH_2CH_2OH]_o} = \frac{\alpha(1-x)\{(1-x)^{(k_5/k_{10})-1} - 1\}}{\{1-(k_5/k_{10})\}} \quad \text{(II)}$$

where $x = 1 - ([C_6F_{13}CH_2CH_2OH]/[C_6F_{13}CH_2CH_2OH]_o)$ is the fractional consumption of $C_6F_{13}CH_2CH_2OH$, α is the yield of $C_6F_{13}CH_2CHO$ from the Cl-atom-initiated oxidation of $C_6F_{13}CH_2CH_2OH$, and k_5 and k_{10} are the rate constants for reactions 5 and 10.

$$Cl + C_6F_{13}CH_2CH_2OH \rightarrow \text{products} \quad (10)$$

The curve through the data in Figure 4 is a fit of eq II to the data, which gives $\alpha = 0.99 \pm 0.08$ and $k_5/k_{10} = 1.18 \pm 0.09$. Using $k_{10} = 1.61 \times 10^{-11}$ [6] gives $k_5 = (1.90 \pm 0.15) \times 10^{-11}$,

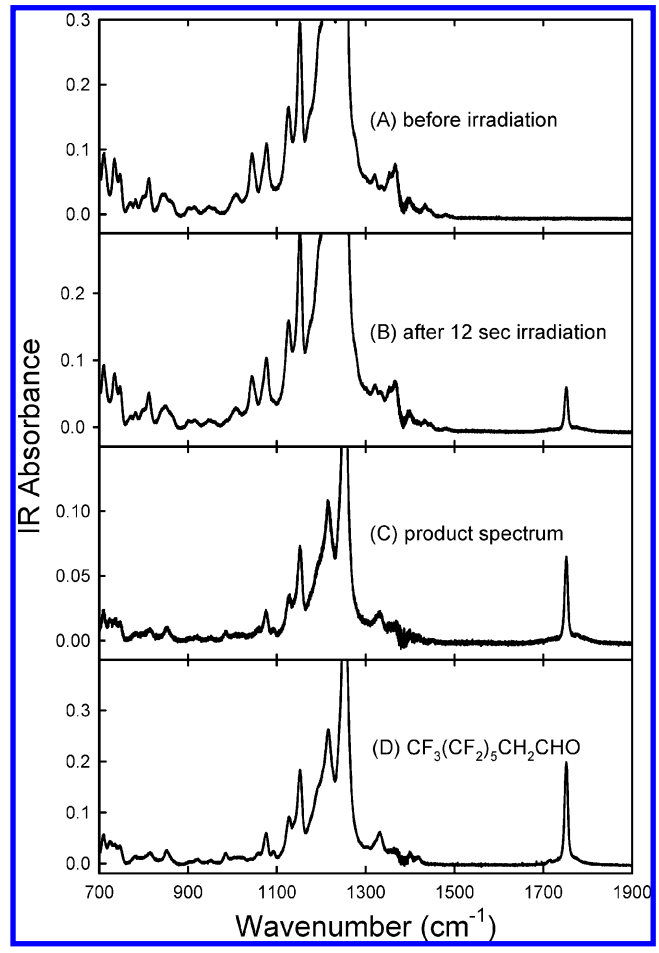

Figure 3. IR spectra acquired before (A) and after (B) a 12 s irradiation of a mixture of 6.8 mTorr of $C_6F_{13}CH_2CH_2OH$ and 100 mTorr of Cl_2 in 700 Torr of air. (C) The product spectrum obtained by subtracting 0.76 of panel (A) from panel (B). A reference spectrum of $C_6F_{13}CH_2CHO$ is given in panel (D).

which is in good agreement with the value of $k_5 = (1.84 \pm 0.22) \times 10^{-11}$ cm^3 molecule^{-1} s^{-1} given in section 3.1. The rate constant ratio $k_5/k_{10} = 1.18 \pm 0.09$ is indistinguishable from the rate constant ratios $k(Cl + C_4F_9CH_2CHO)/k(Cl + C_4F_9CH_2CH_2OH) = 1.14 \pm 0.05$[23] and $k(Cl + C_8F_{17}CH_2CHO)/k(Cl + C_8F_{17}CH_2CH_2OH) = 1.08 \pm 0.07$.[14] The reactivity of $C_nF_{2n+1}CH_2CHO$ does not appear to be sensitive to the size of the C_nF_{2n+1} group.

The observed formation of $C_6F_{13}CH_2CHO$ in a yield which is indistinguishable from 100% is consistent with previous findings that CF_3CH_2CHO, $C_4F_9CH_2CHO$, and $C_8F_{17}CH_2CHO$ are formed in essentially 100% yields from $CF_3CH_2CH_2OH$, $C_4F_9CH_2CH_2OH$, and $C_8F_{17}CH_2CH_2OH$, respectively.[14,23,24] It is clear that reaction 10a proceeds predominantly via hydrogen abstraction from the terminal carbon atom

$$Cl + C_6F_{13}CH_2CH_2OH \rightarrow C_6F_{13}CH_2CHOH + HCl \quad (10a)$$

$$C_6F_{13}CH_2CHOH + O_2 \rightarrow C_6F_{13}CH_2CHO + HO_2 \quad (11)$$

3.4. Formation of $C_6F_{13}CHO$ in the Chlorine-Atom-Initiated Oxidation of $C_6F_{13}CH_2CHO$. Following the UV irradiation of mixtures of 3.1−3.9 mTorr of $C_6F_{13}CH_2CHO$, 100

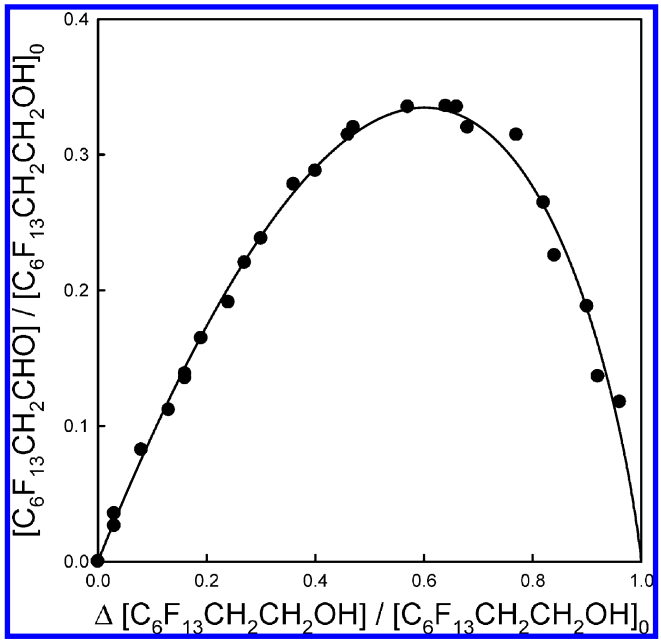

Figure 4. Concentration of $C_6F_{13}CH_2CHO$ (normalized to the initial $C_6F_{13}CH_2CH_2OH$ concentration) versus the fractional consumption of $C_6F_{13}CH_2CH_2OH$ observed following the UV irradiation of $C_6F_{13}CH_2CH_2OH/Cl_2$ mixtures in 700 Torr of air.

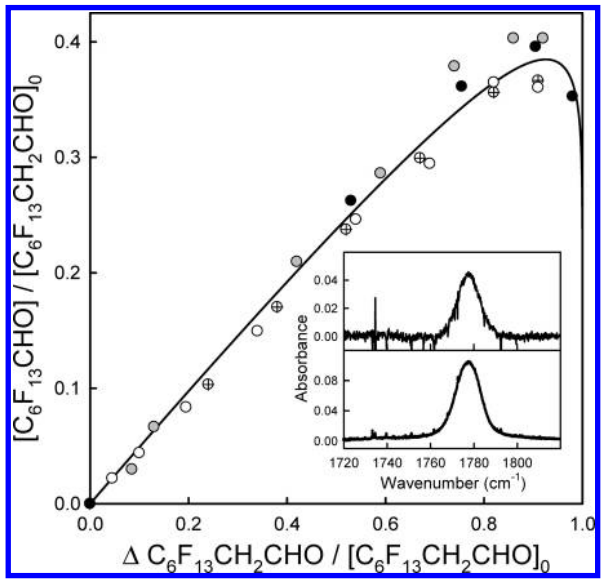

Figure 5. Concentration of $C_6F_{13}CHO$ (normalized to the initial $C_6F_{13}CH_2CHO$ concentration) versus the fractional consumption of $C_6F_{13}CH_2CHO$ observed following the UV irradiation of $C_6F_{13}CH_2CHO/Cl_2/O_2/N_2$ mixtures with $[O_2] = 5$ (open symbols), 10 (crossed symbols), 140 (gray symbols), or 700 Torr (filled symbols) at a total pressure of 700 Torr made up with N_2 as appropriate. The inset shows the IR absorption band centered at 1777 cm^{-1} attributed at $C_6F_{13}CHO$ (top panel) and the reference spectrum of C_4F_9CHO (bottom panel).

mTorr of Cl_2, and 5−700 Torr of O_2 in 700 Torr of total pressure made up as appropriate with N_2, a product with an infrared absorption band centered at 1777 cm^{-1} was observed. The inset in Figure 5 compares this IR feature to that of C_4F_9CHO from our reference library. We do not have a reference spectrum for $C_6F_{13}CHO$, but given the similarity of the spectra shown in the inset in Figure 5 and the expectation that $C_6F_{13}CHO$ will be a product formed in the system, we ascribe the product feature at 1777 cm^{-1} to $C_6F_{13}CHO$. $C_6F_{13}CHO$ was quantified by assuming that its carbonyl feature has the same integrated absorption intensity as C_4F_9CHO (9.27×10^{-18} cm molecule^{-1} [28]). Figure 5 shows a plot of the observed formation of $C_6F_{13}CHO$ versus the consumption of $C_6F_{13}CH_2CHO$. There was no discernible effect of $[O_2]$ over the range of 5−700 Torr on the $C_6F_{13}CHO$ yield. The curve through the data in Figure 5 is a fit of an expression similar to eq II to the data which gives the molar yield of $C_6F_{13}CHO$ in the system, $\alpha' = 0.493 \pm 0.042$ and $k_{12}/k_5 = 0.095 \pm 0.036$.

$$Cl + C_6F_{13}CHO \rightarrow C_6F_{13}CO + HCl \quad (12)$$

The rate constant ratio $k_{12}/k_5 = 0.095 \pm 0.036$ can be combined with $k_5 = (1.84 \pm 0.22) \times 10^{-11}$ (see section 3.1) to give $k_{12} = (1.75 \pm 0.70) \times 10^{-12}$ cm^3 molecule^{-1} s^{-1}. This result is consistent with the previous measurements of $k_{12} = (2.8 \pm 0.7) \times 10^{-12}$ and $(2.1 \pm 0.5) \times 10^{-12}$ cm^3 molecule^{-1} s^{-1} by Solignac et al.[29] and Sulbaek Andersen et al.,[30] respectively.

The formation of $C_6F_{13}CHO$ is consistent with the following reactions occurring in the system

$$Cl + C_6F_{13}CH_2CHO \rightarrow C_6F_{13}CH_2CO + HCl \quad (5a)$$

$$C_6F_{13}CH_2CO + M \rightarrow C_6F_{13}CH_2 + CO + M \quad (13)$$

$$C_6F_{13}CH_2CO + O_2 + M \rightarrow C_6F_{13}CH_2C(O)O_2 + M \quad (14)$$

$$C_6F_{13}CH_2C(O)O_2 + HO_2 + M \rightarrow C_6F_{13}CH_2C(O)OH + O_3 + M \quad (15)$$

$$2C_6F_{13}CH_2C(O)O_2 \rightarrow 2C_6F_{13}CH_2CO_2 + O_2 + M \quad (16)$$

$$C_6F_{13}CH_2CO_2 + M \rightarrow C_6F_{13}CH_2 + CO_2 + M \quad (17)$$

$$C_6F_{13}CH_2 + O_2 + M \rightarrow C_6F_{13}CH_2O_2 + M \quad (18)$$

$$2C_6F_{13}CH_2O_2 \rightarrow 2C_6F_{13}CH_2O + O_2 \quad (19)$$

$$C_6F_{13}CH_2O + O_2 \rightarrow C_6F_{13}CHO + HO_2 \quad (20)$$

In addition to $C_6F_{13}CHO$, we would expect the formation of $C_6F_{13}CH_2C(O)OH$ (via reaction 15) and $C_6F_{13}CH_2OH$ and $C_6F_{13}CH_2OOH$ (via the molecular channel of reaction 19 [not shown] and via the $C_6F_{13}CH_2O_2 + HO_2$ reaction) products in the system.

3.5. Atmospheric Fate of $C_6F_{13}CH_2C(O)$ and $C_6F_{13}C(O)$ Radicals. In addition to $C_6F_{13}CHO$, the UV irradiation of $C_6F_{13}CH_2CHO/Cl_2/O_2/N_2$ mixtures led to the formation of CO_2, CO, and COF_2 as observed products. Figure 6 shows plots of the formation of CO_2, CO, and COF_2 versus the fractional consumption of $C_6F_{13}CH_2CHO$. As seen from Figure 6, there was no obvious systematic effect of the oxygen concentration (varied over the range of 5−700 Torr) on the observed product formation. The formation of CO_2 increased linearly with the consumption of $C_6F_{13}CH_2CHO$; the line through the data gives a molar yield of 63 ± 5%. In contrast, the yields of CO and COF_2 were distinctly nonlinear, starting at zero for small $C_6F_{13}CH_2CHO$ consumptions and increasing sharply at high

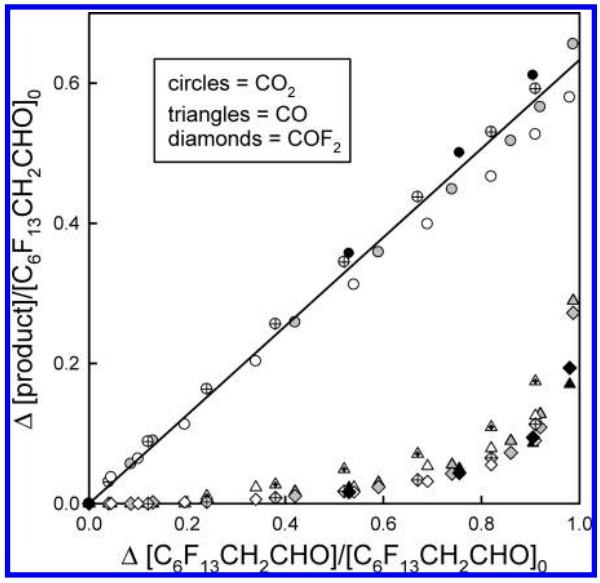

Figure 6. Concentrations of CO_2 (circles), CO (triangles), and COF_2 (diamonds) normalized to the initial $C_6F_{13}CH_2CHO$ concentration versus the fractional consumption of $C_6F_{13}CH_2CHO$ observed following the UV irradiation of $C_6F_{13}CH_2CHO/Cl_2/O_2/N_2$ mixtures with $[O_2] = 5$ (open symbols), 10 (crossed symbols), 140 (gray symbols), or 700 Torr (filled symbols) at a total pressure of 700 Torr made up with N_2 as appropriate. The COF_2 data have been divided by a factor of 5; see text for details.

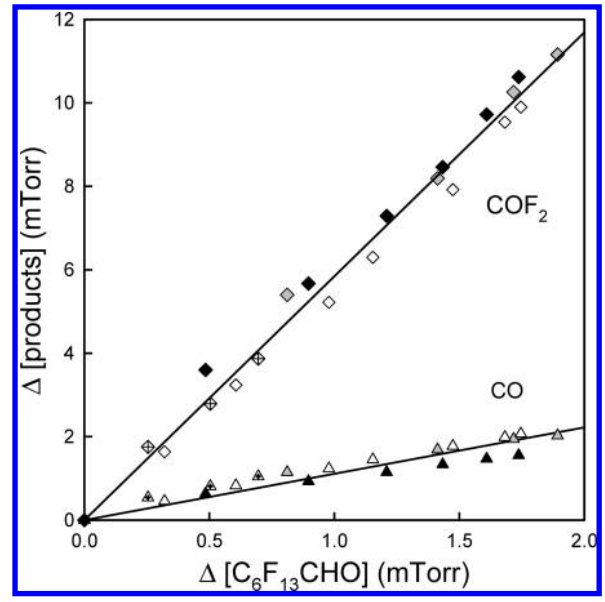

Figure 7. Formation of CO (triangles) and COF_2 (diamonds) versus the loss of $C_6F_{13}CHO$ observed following the UV irradiation of $C_6F_{13}CH_2CHO/Cl_2/O_2/N_2$ mixtures with $[O_2] = 5$ (open symbols), 10 (crossed symbols), 140 (gray symbols), or 700 Torr (filled symbols) at a total pressure of 700 Torr made up with N_2 as appropriate.

(>90%) consumptions. The molar yield of COF_2 was substantially larger than that for CO, and to display the two species on the same scale in Figure 6, we have divided the COF_2 yield by a factor of 5.

The yields of CO_2, CO, and COF_2 shown in Figure 6 contain information concerning the fate of $C_6F_{13}CH_2C(O)$ and $C_6F_{13}C(O)$ radicals in the system. As indicated in the previous section, the reaction of chlorine atoms with $C_6F_{13}CH_2CHO$ gives $C_6F_{13}CH_2C(O)$ radicals, which can either add O_2, leading to the formation of CO_2, or decompose, leading to the formation of CO. The observation of a substantial yield of CO_2 and the absence of CO for low conversions of $C_6F_{13}CH_2CHO$ shows that even in the presence of 5 Torr of O_2, the addition of O_2 (reaction 14) dominates decomposition (reaction 13) as the loss mechanism for $C_6F_{13}CH_2C(O)$ radicals at 296 K. Reaction 13 is a unimolecular decomposition, and its rate will decrease more rapidly than that of reaction 14 at lower temperatures. Hence, we conclude that the sole atmospheric fate of $C_6F_{13}CH_2C(O)$ radicals is addition of O_2 to give the corresponding acyl peroxy radical.

As seen from Figure 5, for $C_6F_{13}CH_2CHO$ consumptions greater than approximately 60%, there is a noticeable decrease in the apparent yield of $C_6F_{13}CHO$, which we attribute to loss via reaction with chlorine atoms. This reaction produces $C_6F_{13}C(O)$ radicals which can either add O_2 or decompose.

$$Cl + C_6F_{13}CHO \rightarrow C_6F_{13}CO + HCl \qquad (12a)$$

$$C_6F_{13}C(O) + O_2 + M \rightarrow C_6F_{13}C(O)O_2 + M \qquad (21)$$

$$C_6F_{13}C(O) + M \rightarrow C_6F_{13} + CO + M \qquad (22)$$

As seen from Figure 6, for $C_6F_{13}CH_2CHO$ consumptions > 60%, there is a large increase in the yield of both CO and COF_2, but there is no discernible change in the yield of CO_2, leading to the conclusion that even in the presence of 700 Torr of O_2, reaction 22 dominates the fate of $C_6F_{13}C(O)$ radicals.

Subtracting the observed $C_6F_{13}CHO$ concentration in a given experiment from the expected concentration calculated from the measured $C_6F_{13}CH_2CHO$ loss and the molar yield of $C_6F_{13}CHO$ of 0.493 ± 0.042 (see section 3.4) gives an estimate of the loss of $C_6F_{13}CHO$ via reaction 12a. Figure 7 shows a plot of the observed formation of COF_2 and CO versus the calculated loss of $C_6F_{13}CHO$. The lines through the data give yields of COF_2 and CO of 581 ± 63 and 129 ± 17%, respectively, where the uncertainties include two standard deviations from the regressions. The yield of COF_2 somewhat exceeds the value of 500% expected from the "unzipping" reactions,[7] which will lead to conversion of $-CF_2-$ groups in the $CF_3(CF_2)_5$ radicals produced in reaction 22 via the sequence

$$CF_3(CF_2)_x + O_2 + M \rightarrow CF_3(CF_2)_xO_2 + M \qquad (23)$$

$$2CF_3(CF_2)_xO_2 \rightarrow CF_3(CF_2)_xO + O_2 \qquad (24)$$

$$CF_3(CF_2)_xO + M \rightarrow CF_3(CF_2)_{x-1} + COF_2 \qquad (25)$$

The yield of CO somewhat exceeds the value of 100% expected if decomposition was the sole fate of $C_6F_{13}C(O)$ radicals. The ratio of the COF_2 to CO yield is 4.50 ± 0.77 and is consistent with expectations if decomposition via reaction 22 is the sole fate of $C_6F_{13}C(O)$ radicals. The product yields of CO and COF_2 suggest that even in the presence of 700 Torr of O_2, the dominant fate of $C_6F_{13}C(O)$ radicals is decomposition.

Solignac et al.[29] have reported a 52% CO yield in the chlorine-initiated oxidation of the alcohol $C_6F_{13}CH_2OH$ in air, which they attributed to the chlorine-initiated oxidation of the aldehyde $C_6F_{13}CHO$. Hurley et al.[31] studied the chlorine-atom-initiated oxidation of $C_nF_{2n+1}CHO$ ($n = 1, 2, 3, 4$) and concluded that in 1 atm of air at 298 K, decomposition accounts for 1, 50, 79, and 88% of the fate of $C_nF_{2n+1}C(O)$ radicals for $n = 1, 2, 3$, and 4, respectively. Waterland and Dobbs[32] used ab initio

calculations to show that the activation energy barrier for unimolecular decomposition of the first three members of the $C_nF_{2n+1}C(O)$ series decreases progressively from 8.8 kcal mol^{-1} for CF_3CO to 5.8 kcal mol^{-1} for C_3F_7CO. The observation in the present work that decomposition is the dominant fate of $C_6F_{13}C(O)$ radicals in 700 Torr of N_2/O_2 mixtures at 296 K is consistent with expectations based upon the available experimental and theoretical data for smaller members of the series. If, based upon the trend of the results from Waterland and Dobbs,[32] we assume an activation barrier of 4−5 kcal mol^{-1} for reaction 22, then the rate of reaction 22 will slow by approximately a factor of 10−20 upon moving from 296 K to a temperature of 220 K representative of the upper troposphere. Given the fact that at 296 K we observe no effect upon increasing the partial oxygen pressure by a factor of 5 from that present in 1 atm of air (i.e., from $[O_2] = 140$ to 700 Torr), it seems likely that decomposition dominates the atmospheric fate of $C_6F_{13}C(O)$ radicals.

4. Implications for Atmospheric Chemistry

The goal of this work was to improve our understanding of the atmospheric chemistry of fluorinated aldehydes, in general, and $C_6F_{13}CH_2CHO$, in particular. We show that $C_6F_{13}CH_2CHO$ is formed in essentially 100% yield during the chlorine-atom, and by inference OH-radical, -initiated oxidation of $C_6F_{13}CH_2CH_2OH$. We provide the first measurements of $k(Cl + C_6F_{13}CH_2CHO) = (1.84 \pm 0.22) \times 10^{-11}$ and $k(OH + C_6F_{13}CH_2CHO) = (2.15 \pm 0.26) \times 10^{-12}$ cm^3 molecule^{-1} s^{-1} in 700 Torr of N_2, or air, diluent at 296 ± 2K. The results are consistent with the database[14,21,23,24,26] for reactions of $C_nF_{2n+1}CH_2CHO$ aldehydes. Combining $k(OH + C_6F_{13}CH_2CHO) = 2.15 \times 10^{-12}$ cm^3 molecule^{-1} s^{-1} with an estimate of the 24 h global average OH concentration of 1.0×10^6 cm^{-3} gives a lifetime of approximately 5 days for $C_6F_{13}CH_2CHO$ with respect to reaction with OH. The lifetime of $C_6F_{13}CH_2CHO$ with respect to photolysis is approximately 10−15 days.[15,16] Hence, photolysis and reaction with OH radicals are competing atmospheric fates for $C_6F_{13}CH_2CHO$.

We show here that the oxidation of $C_6F_{13}CH_2CHO$ gives the perfluoroaldehyde $C_6F_{13}CHO$. The gas-phase atmospheric oxidation of perfluoroaldehydes proceeds via both photolysis and reaction with OH radicals, with photolysis believed to be the more important loss mechanism. Photolysis of $C_nF_{2n+1}CHO$ gives C_nF_{2n+1} and HCO radicals, while reaction with OH gives $C_nF_{2n+1}C(O)$ radicals. As discussed in section 3.5, decomposition and addition of O_2 are competing atmospheric fates of $C_nF_{2n+1}C(O)$ radicals. For small members of the series, the addition of O_2 dominates. We show here that for $C_6F_{13}C(O)$ and larger members of the series, decomposition is the dominant process. Interest in the atmospheric chemistry of fluorinated alcohols and aldehydes is driven by a desire to understand their potential role in the formation of perfluorocarboxylic acids. From the perspective of understanding perfluorocarboxylic acid formation, the distinction between photolysis and reaction with O_2 as competing fates for $C_6F_{13}CHO$, and larger aldehydes, is moot as both processes lead to the rapid formation of C_6F_{13} radicals and CO.

Three mechanisms have been proposed by which perfluorinated aldehydes can be converted into perfluorocarboxylic acids in the atmosphere. First is reaction of $C_nF_{2n+1}CHO$ with OH radicals, addition of O_2 to give the acylperoxy radical, followed by reaction with HO_2 radicals[33]

$$C_nF_{2n+1}CHO + OH \rightarrow C_nF_{2n+1}C(O) + H_2O$$

$$C_nF_{2n+1}C(O) + O_2 + M \rightarrow C_nF_{2n+1}C(O)O_2 + M$$

$$C_nF_{2n+1}C(O)O_2 + HO_2 \rightarrow C_nF_{2n+1}C(O)OH + O_3$$

Second is conversion of $C_nF_{2n+1}CHO$ into C_nF_{2n+1} radicals (via photolysis or reaction with OH), which add O_2 and react with CH_3O_2 radicals to give $C_{n-1}F_{2n-1}CF_2OH$, which then eliminates HF to give the acyl fluoride $C_{n-1}F_{2n-1}C(O)F$, which in turn reacts with water[7]

$$C_nF_{2n+1}CHO + h\nu \rightarrow C_nF_{2n+1} + HCO$$

$$C_nF_{2n+1} + O_2 + M \rightarrow C_nF_{2n+1}O_2 + M$$

$$C_nF_{2n+1}O_2 + CH_3O_2 \rightarrow C_{n-1}F_{2n-1}CF_2OH + HCHO + O_2$$

$$C_{n-1}F_{2n-1}CF_2OH \rightarrow C_{n-1}F_{2n-1}C(O)F + HF$$

$$C_{n-1}F_{2n-1}C(O)F + H_2O \rightarrow C_{n-1}F_{2n-1}C(O)OH + HF$$

Third is hydration of $C_nF_{2n+1}CHO$ to give a gem-diol, which reacts with OH[34]

$$C_nF_{2n+1}CHO + H_2O \rightarrow C_nF_{2n+1}CH(OH)_2$$

$$C_nF_{2n+1}CH(OH)_2 + OH \rightarrow C_nF_{2n+1}C(OH)_2 + H_2O$$

$$C_nF_{2n+1}C(OH)_2 + O_2 \rightarrow C_nF_{2n+1}C(O)OH + HO_2$$

We show that decomposition dominates the atmospheric fate of $C_6F_{13}C(O)$ radicals. The present work combined with previous experimental[29,31] and theoretical[32] investigations indicates that the first mechanism is not a significant environmental source of perfluorocarboxylic acids in the oxidation of $C_6F_{13}CHO$ and larger perfluoroaldehydes. Additional work is needed to clarify the importance of the second and third mechanisms as potential sources of perfluorocarboxylic acids.

Finally, it is germane to note that in addition to the uncertainties in their sources, the ultimate fate of perfluorocarboxylic acids is also unclear. The only mechanism that has been established for the destruction of perfluorocarboxylic acids in the environment is the gas-phase reaction with OH radicals,[35] which leads to conversion into CO_2 and HF. However, the rate of this reaction is sufficiently slow that only approximately 10% of the perfluorocarboxylic acids present in the gas phase will react while the remaining 90% will be transferred by wet and dry deposition into the hydrosphere. McMurdo et al.[36] have suggested that aerosol-mediated transport of perfluorocarboxylic acids from the water bodies back into the atmosphere might be significant. If perfluorocarboxylic acids circulate back to the gas phase, they will be exposed to further attack and degradation by OH radicals, although the overall efficiency of such circulation and additional degradation is unclear. Further work is needed to understand the sources and sinks of perfluorocarboxylic acids.

Acknowledgment. The authors thank Rob Waterland for providing the $C_6F_{13}CH_2CHO$ sample. G.A.A. and M.S.C. thank

DuPont de Nemours (USA), CONICET, SeCyT-UNC, and ANPCyT (Argentina) for research grants which made this work possible.

References and Notes

(1) Ellis, D. A.; Moody, C. A.; Mabury, S. A. In *Handbook of Environmental Chemistry: Part N, Organofluorines*; Nielson, A., Ed.; Springer-Verlag: Heidelberg, Germany, 2002; p 103.

(2) Scott, B. F.; Spencer, C.; Moody, C. A.; Mabury, S. A.; MacTavish, D.; Muir, D. C. G. Poster presented at the 13th Annual SETAC Europe Meeting, Hamburg, Germany, 2003.

(3) Martin, J. W.; Mabury, S. A.; Solomon, K. R.; Muir, D. C. G. *Environ. Toxicol. Chem.* **2003**, *22*, 196–204.

(4) Martin, J. W.; Whittle, D. M.; Muir, D. C. G.; Mabury, S. A. *Environ. Sci. Technol.* **2004**, *38*, 5379–5385.

(5) Martin, J. W.; Smithwick, M. M.; Braune, B. M.; Hekstra, P. F.; Muir, D. C. G.; Mabury, S. A. *Environ. Sci. Technol.* **2004**, *38*, 373–380.

(6) Ellis, D. A.; Martin, J. W.; Mabury, S. A.; Hurley, M. D.; Andersen, M. P. S.; Wallington, T. J. *Environ. Sci. Technol.* **2003**, *37*, 3816–3820.

(7) Ellis, D. A.; Martin, J. W.; De Silva, A. O.; Mabury, S. A.; Hurley, M. D.; Andersen, M. P. S.; Wallington, T. J. *Environ. Sci. Technol.* **2004**, *38*, 3316–3321.

(8) Stock, N. L.; Lau, F. K.; Ellis, D. A.; Martin, J. W.; Muir, D. C. G.; Mabury, S. A. *Environ. Sci. Technol.* **2004**, *38*, 991–996.

(9) Shoeib, M.; Harner, T.; Vlahos, P. *Environ. Sci. Technol.* **2006**, *40*, 7577–7583.

(10) Jahnke, A.; Ahrens, L.; Ebinghaus, R.; Temme, C. *Environ. Sci. Technol.* **2007**, *41*, 745–752.

(11) Jahnke, A.; Berger, U.; Ebinghaus, R.; Temme, C. *Environ. Sci. Technol.* **2007**, *41*, 3055–3061.

(12) Kelly, T.; Bossoutrot, V.; Magneron, I.; Wirtz, K.; Treacy, J.; Mellouki, A.; Sidebottom, H.; Le Bras, G. *J. Phys. Chem. A* **2005**, *109*, 347–355.

(13) Hurley, M. D.; Ball, J. C.; Wallington, T. J.; Sulbaek Andersen, M. P.; Ellis, D. A.; Martin, J. W.; Mabury, S. A. *J. Phys. Chem. A* **2004**, *108*, 5635–5642.

(14) Chiappero, M. S.; Argüello, G. A.; Hurley, M. D.; Wallington, T. J. *Chem. Phys. Lett.* **2008**, *461*, 198–202.

(15) Chiappero, M. S.; Malanca, F. E.; Argüello, G. A.; Wooldridge, S. T.; Hurley, M. D.; Ball, J. C.; Wallington, T. J.; Waterland, R. L.; Buck, R. C. *J. Phys. Chem. A* **2006**, *110*, 11944–11953.

(16) Solignac, G.; Mellouki, A.; Le Bras, G.; Yujing, M.; Sidebottom, H. *Phys. Chem. Chem. Phys.* **2007**, *9*, 4200–4210.

(17) Wallington, T. J.; Gierczak, C. A.; Ball, J. C.; Japar, S. M. *Int. J. Chem. Kinet.* **1989**, *21*, 1077–1089.

(18) Atkinson, R. J. *Phys. Chem. Ref. Data* **1989**, 1–246, Monograph 1.

(19) Wine, P. H.; Semmes, D. H. *J. Phys. Chem.* **1983**, *87*, 3572–3578.

(20) Atkinson, R.; Baulch, D. L.; Cox, R. A.; Crowley, J. N.; Hampson, R. F.; Hynes, R. G.; Jenkin, M. E.; Rossi, M. J.; Troe, J. *Atmos. Chem. Phys.* **2006**, *6*, 3625–4055.

(21) Kelly, T.; Bossoutrot, V.; Magneron, I.; Wirtz, K.; Treacy, J.; Mellouki, A.; Sidebottom, H.; Le Bras, G. *J. Phys. Chem. A* **2005**, *109*, 347–355.

(22) Wallington, T. J.; Haryanto, A.; Hurley, M. D. *Chem. Phys. Lett.* **2006**, *432*, 57–61.

(23) Hurley, M. D.; Misner, J. A.; Ball, J. C.; Wallington, T. J.; Ellis, D. A.; Martin, J. W.; Mabury, S. A. *J. Phys. Chem. A* **2005**, *109*, 9816–9826.

(24) Sulbaek Andersen, M. P.; Nielsen, O. J.; Hurley, M. D.; Ball, J. C.; Wallington, T. J.; Ellis, D. A.; Martin, J. W.; Mabury, S. A. *J. Phys. Chem. A* **2005**, *109*, 1849–1856.

(25) Calvert, J. G.; Atkinson, R.; Kerr, J. A.; Madronich, S.; Moortgat, G. K.; Wallington, T. J.; Yarwood, G. *Mechanisms of the Atmospheric Oxidation of the Alkenes*; Oxford University Press: New York, 2000;, ISBN 0-19-513177-0.

(26) Sellevåg, S. R.; Kelly, T.; Sidebottom, H.; Nielsen, C. *Phys. Chem. Chem. Phys.* **2004**, *6*, 1243–1252.

(27) Meagher, R. J.; McIntosh, M. E.; Hurley, M. D.; Wallington, T. J. *Int. J. Chem. Kinet.* **1997**, *29*, 619–625.

(28) Hashikawa, Y.; Kawasaki, M.; Waterland, R. L.; Sulbaek Andersen, M. P.; Nielsen, O. J.; Hurley, M. D.; Ball, J. C.; Wallington, T. J. *J. Fluorine Chem.* **2004**, *125*, 1925–1932.

(29) Solignac, G.; Mellouki, A.; Le Bras, G.; Barnes, I.; Benter, Th. *J. Phys. Chem. A* **2006**, *110*, 4450–4457.

(30) Sulbaek Andersen, M. P.; Nielsen, O. J.; Hurley, M. D.; Ball, J. C.; Wallington, T. J.; Stevens, J. E.; Martin, J. W.; Ellis, D. A.; Mabury, S. A. *J. Phys. Chem. A* **2004**, *108*, 5189–5196.

(31) Hurley, M. D.; Ball, J. C.; Wallington, T. J.; Sulbaek Andersen, M. P.; Nielsen; Ellis, D. A.; Martin, J. W.; Mabury, S. A. *J. Phys. Chem. A* **2006**, *110*, 12443–12447.

(32) Waterland, R.; Dobbs, K. *J. Phys. Chem. A* **2007**, *111*, 2555–2562.

(33) Sulbaek Andersen, M. P.; Stenby, C.; Nielsen, O. J.; Hurley, M. D.; Ball, J. C.; Wallington, T. J.; Martin, J. W.; Ellis, D. A.; Mabury, S. A. *J. Phys. Chem. A* **2004**, *108*, 6325–6330.

(34) Sulbaek Andersen, M. P.; Toft, A.; Nielsen, O. J.; Hurley, M. D.; Wallington, T. J.; Chishma, H.; Tonokura, K.; Mabury, S. A.; Martin, J. W.; Ellis, D. A. *J. Phys. Chem. A* **2006**, *110*, 9854–9860.

(35) Hurley, M. D.; Sulbaek Andersen, M. P.; Wallington, T. J.; Ellis, D. A.; Martin, J. W.; Mabury, S. A. *J. Phys. Chem. A* **2004**, *108*, 615–620.

(36) McMurdo, C. J.; Ellis, D. A.; Webster, E.; Butler, J.; Christensen, R. D.; Reid, L. K. *Environ. Sci. Technol.* **2008**, *42*, 3969–3974.

JP101587M